INSTITUTE for NUCLEAR THEORY

NEUTRON SKIN DETERMINATIONS VIA ISOBAR COLLISIONS

HAOJIE XU (徐浩洁)

HUZHOU UNIVERSITY(湖州师范学院)

Intersection of nuclear structure and high−energy nuclear collisions
February 3, 2023

Outline

I. Nuclear structure of isobars

II. How to probe neutron skin thickness and nuclear symmetry energy using isobar collisions

III. Summary

I. Nuclear structure of isobars

Relativistic Heavy ion collisions

Woods-Saxon distributions

$$\rho(r) = \frac{\rho_0}{1 + \exp[(r - R)/a]}$$

$$R = R_0\,[1+\beta_2 Y_2^0(\theta)+\beta_4 Y_4^0(\theta)]$$

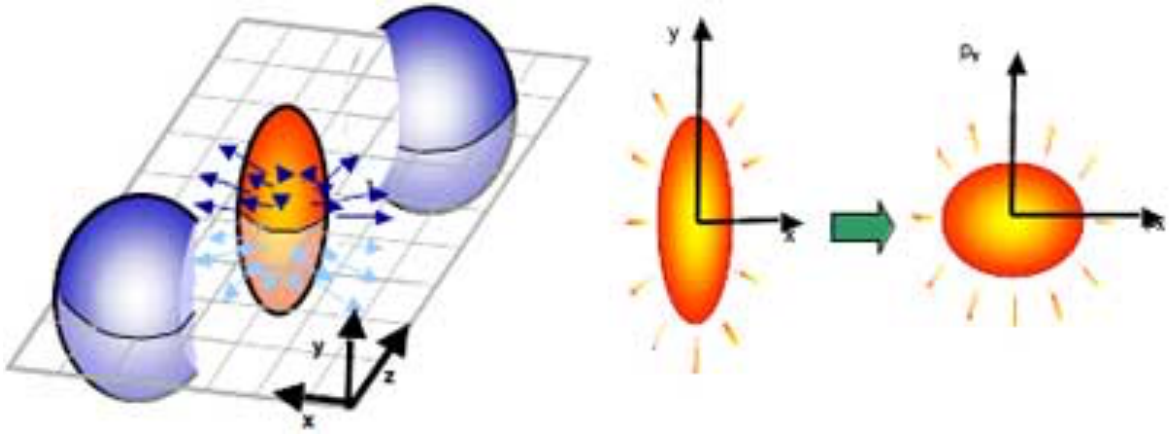

Anisotropic flow,
Flow fluctuations
HBT,
....

Initial geometry

Bulk properties of QGP medium: $\eta/s, \zeta/s, \ldots$

Final observables

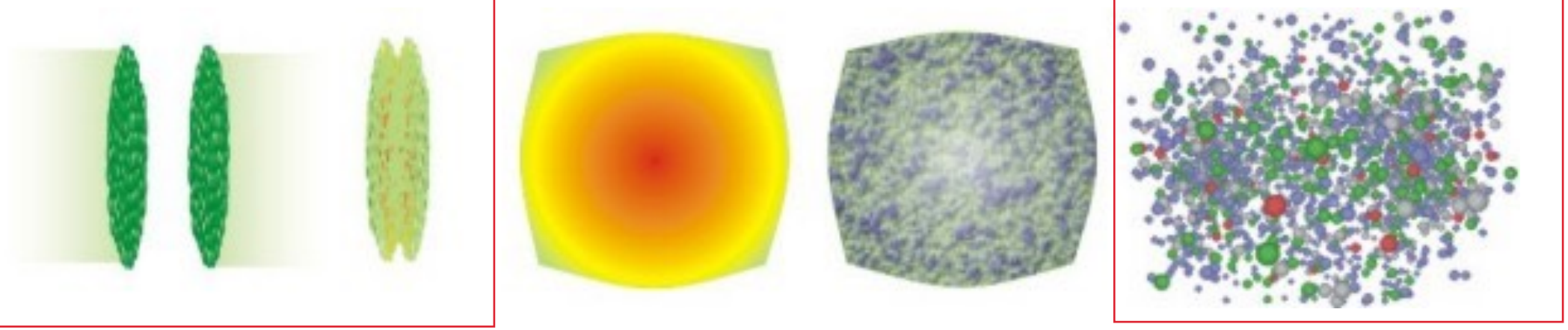

Relativistic isobaric collisions and chiral magnetic effect

Fuqiang Wang's talk

Chiral magnetic effect (CME)

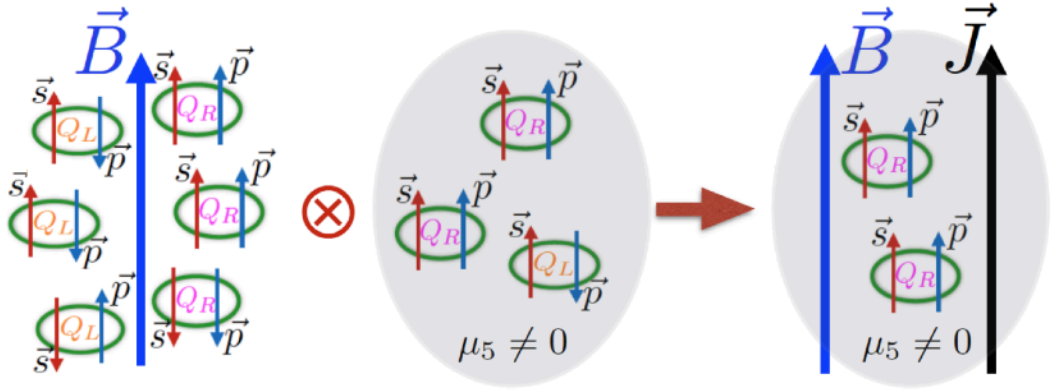

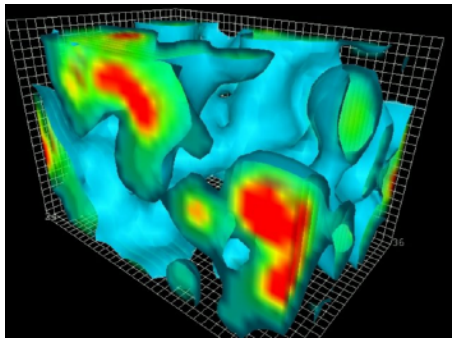

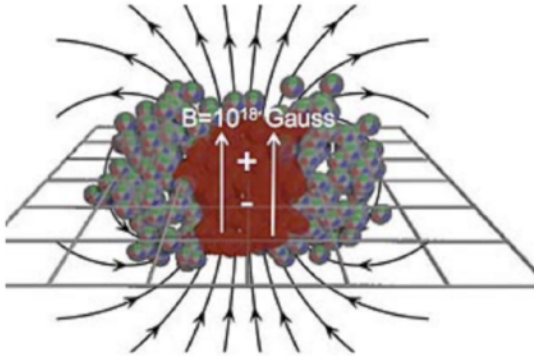

$$\mathbf{J_{cme}} = \sigma_5 \mathbf{B} = \left(\frac{(Qe)^2}{2\pi^2}\mu_5\right)\mathbf{B},$$

D. Kharzeev,et.al., PPNP88, 1(2016)

The isobar collisions was proposed to measure the chiral magnetic effect.

S. Voloshin, PRL105, 172301 (2010)

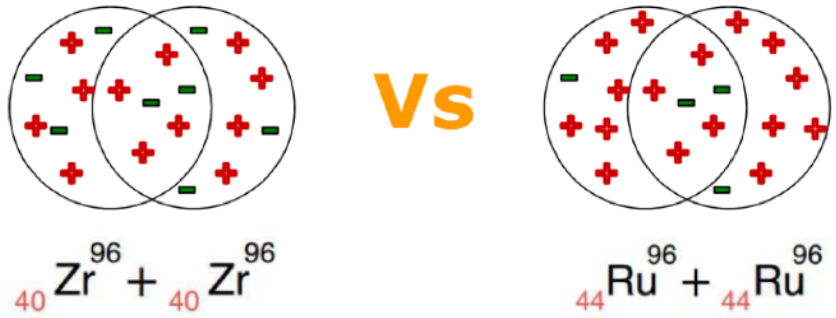

- Same background
- Different magnetic field => different CME signals

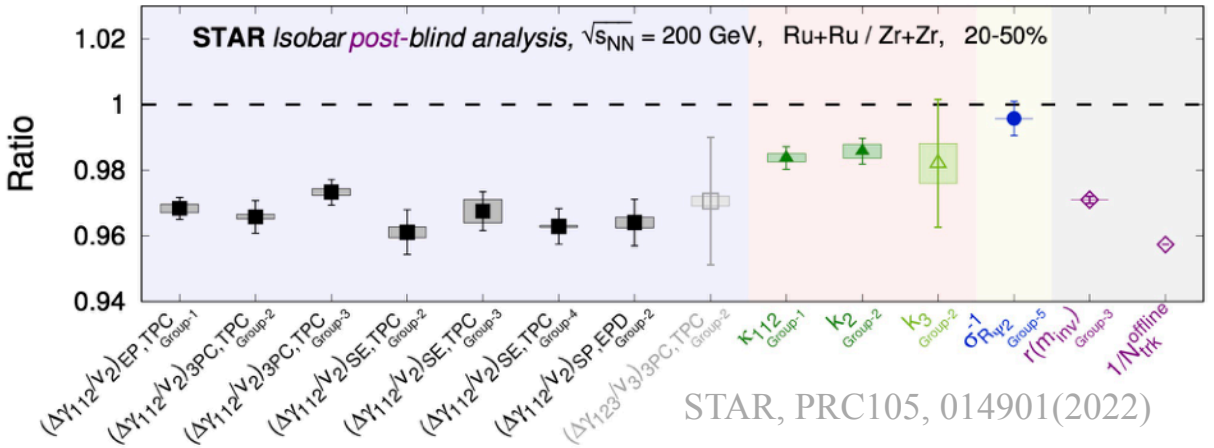

STAR, PRC105, 014901(2022)

Backgrounds are not identical!!!

Haojie Xu

Predictions from charge density distributions

$$\rho = \frac{\rho_0}{1 + \exp\left[\frac{r - R}{a}\right]}$$

	R	a	beta2
Zr	5.02	0.46	0.08/0.217
Ru	5.085	0.46	0.158/0.053

WS parameters extracted from charge density distributions

W. Deng, X. Huang, et.al., PRC94,041901(2016)

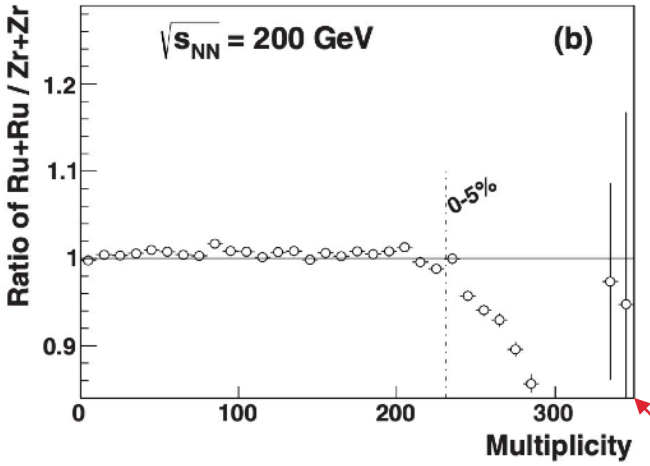

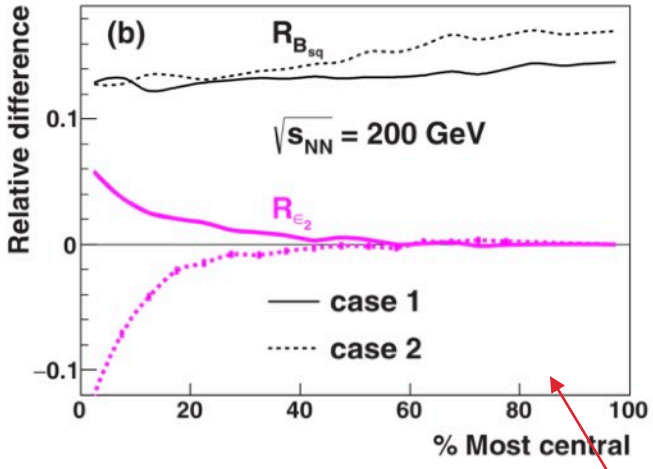

$$\Delta\gamma_{\text{bkg}} = \langle\cos(\varphi_\alpha + \varphi_\beta - 2\Psi_{RP})\rangle = \frac{N_{\text{cluster}}}{N_\alpha N_\beta} \times \langle\cos(\varphi_\alpha + \varphi_\beta - 2\Psi_{\text{cluster}})\rangle \times v_{2,\text{cluster}}$$

Nuclear structure calculation by DFT

- **Charge density ≠ nuclear density.**
- The proton and neutron densities obtained from the energy density functional theory (DFT)

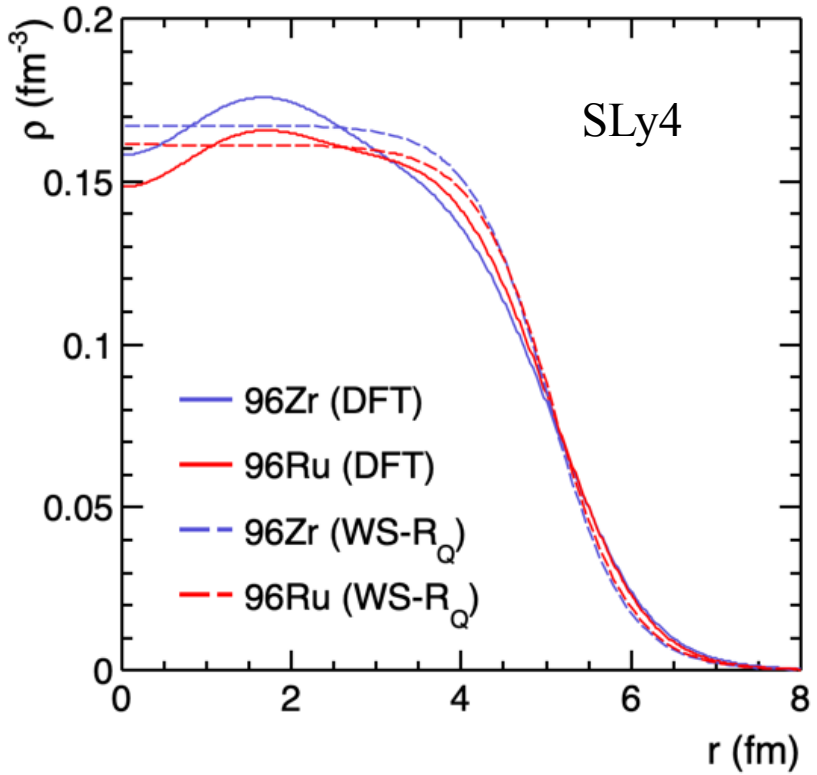

HJX, et.al., PRL121, 022301 (2018)
H. Li, HJX, et.al., PRC98, 054907(2018)

Predictions on isobar differences

Predictions with charge densities

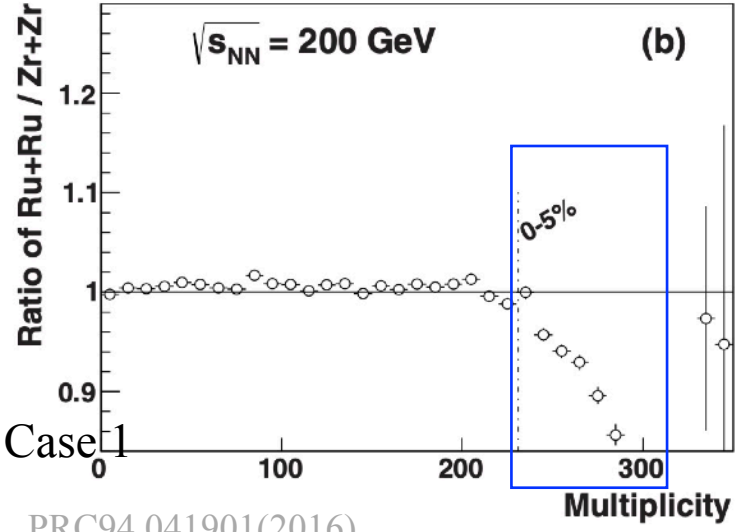

Case 1

W. Deng, et.al., PRC94,041901(2016)

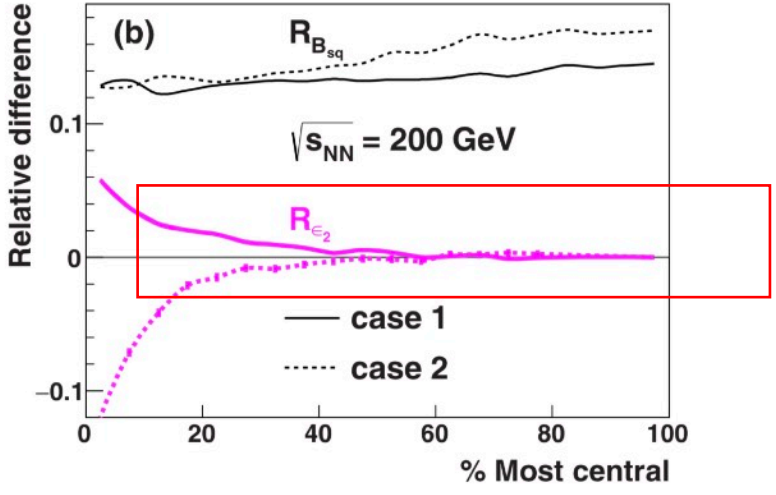

Predictions with DFT densities

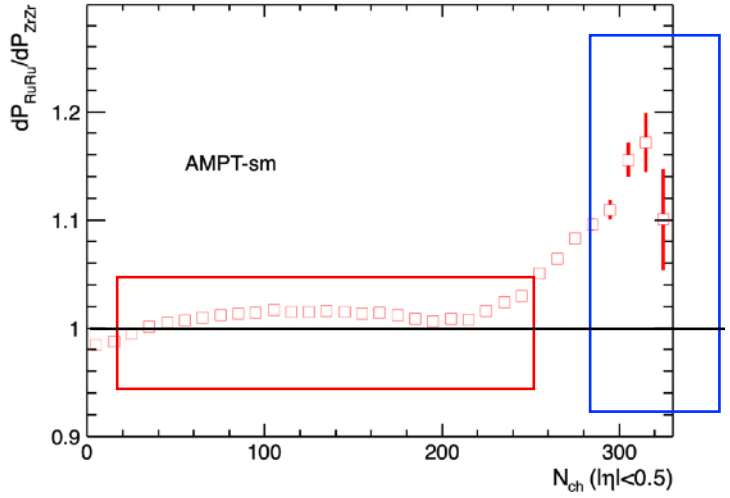

HJX, et.al, PRL121, 022301(2018)
H. Li, HJX, et.al., PRC98, 054907(2018)

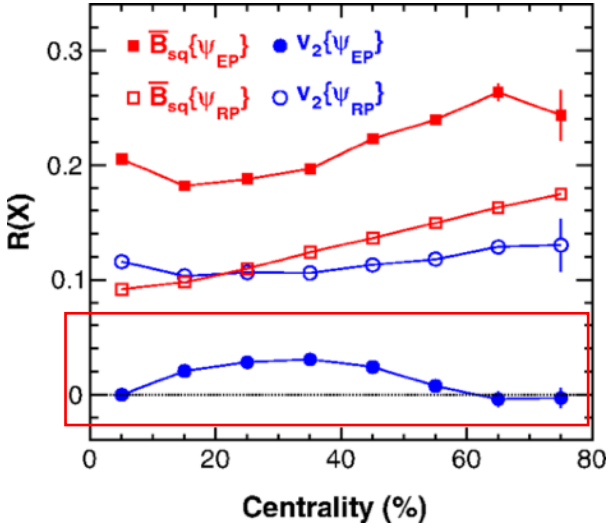

DFT predictions are verified by STAR data

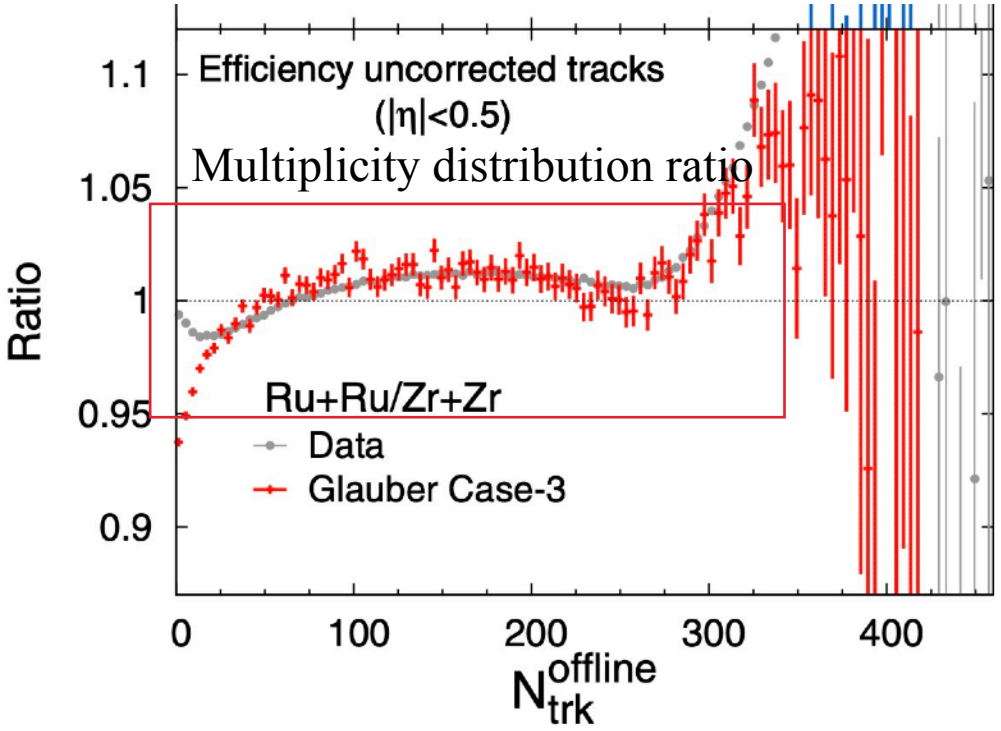

STAR, PRC105, 014901(2022)

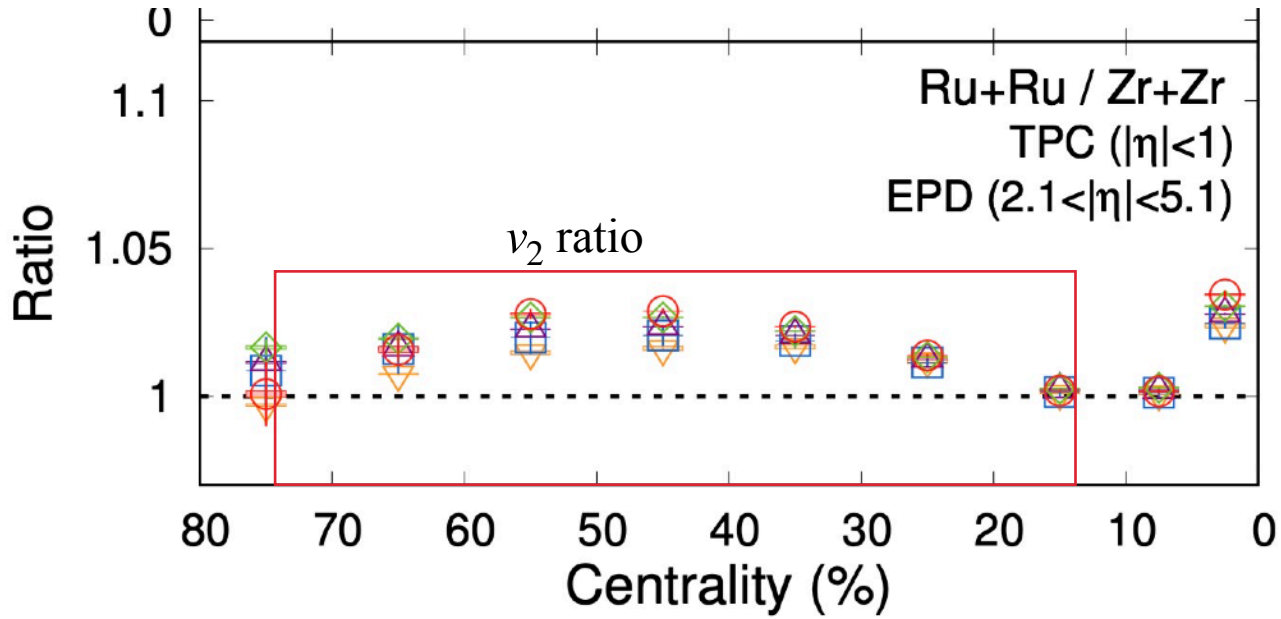

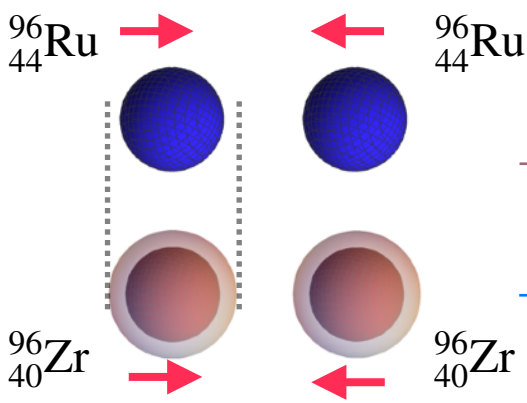

Neutron skin thickness $\Delta r_{np} \equiv \sqrt{\langle r_n^2 \rangle} - \sqrt{\langle r_p^2 \rangle}$

Smaller r, larger density → Larger N_{ch} and $\langle p_T \rangle$

Larger r, smaller density → Smaller N_{ch} and $\langle p_T \rangle$

HJX, et.al., PRL121, 022301 (2018)
H. Li, HJX, et.al., PRC98, 054907 (2018)
HJX, et.al., PLB819, 136453 (2021)

Haojie Xu

Determine the neutron skin type by STAR data

HJX, et.al., PLB819, 136453 (2021)

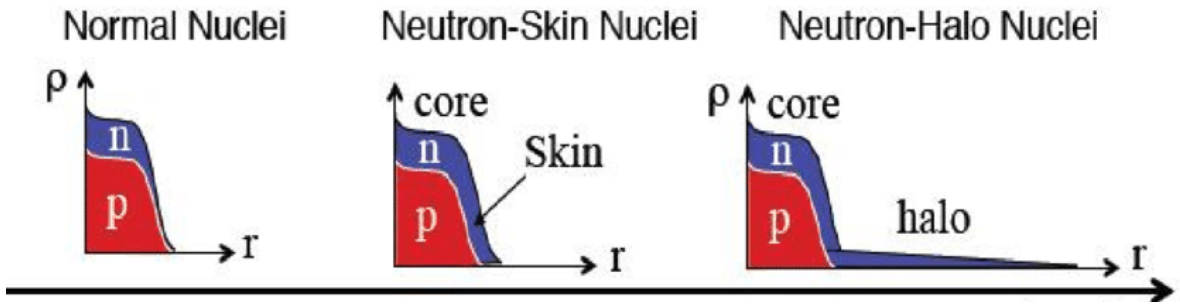

- Neutron-skin nuclei and neutron-halo nuclei for Zr

	^{96}Ru		^{96}Zr	
	R	a	R	a
p	5.085	0.523	5.021	0.523
skin-type n	5.085	0.523	5.194	0.523
halo-type n	5.085	0.523	5.021	0.592

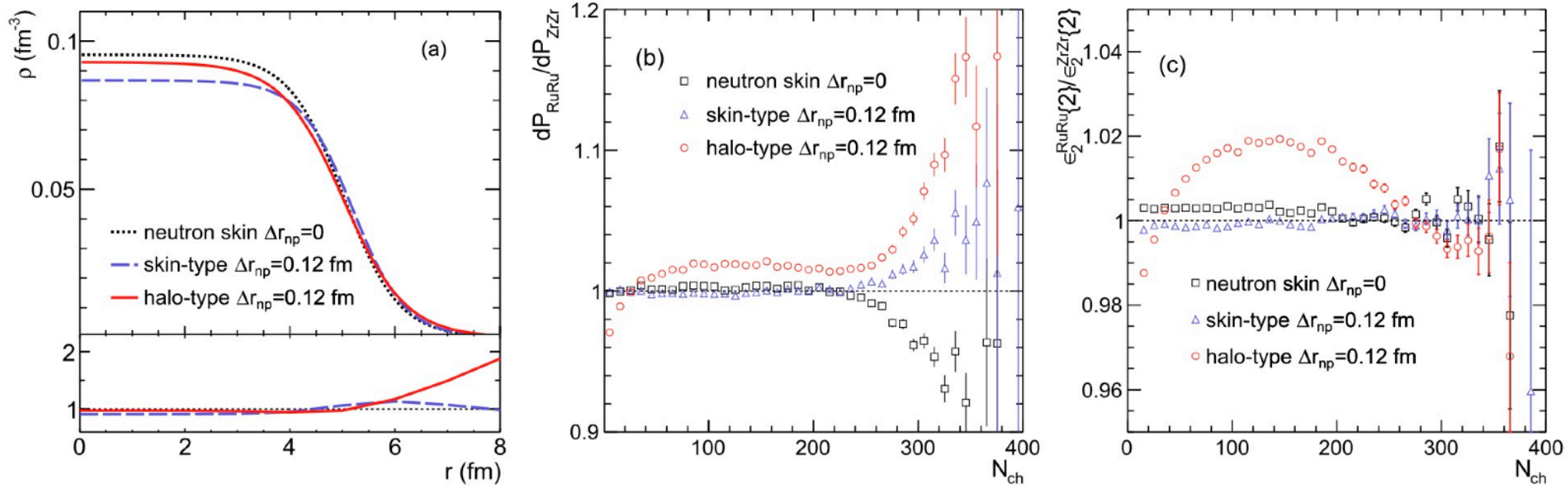

The shapes of the Ru+Ru/Zr+Zr ratios of the multiplicity and eccentricity in mid-central collisions can further distinguish between skin-type and halo-type neutron densities.

Haojie Xu

Photoproduction of di-electrons in peripheral isobar collisions

S. Lin, et.al, arXiv:2210.05106

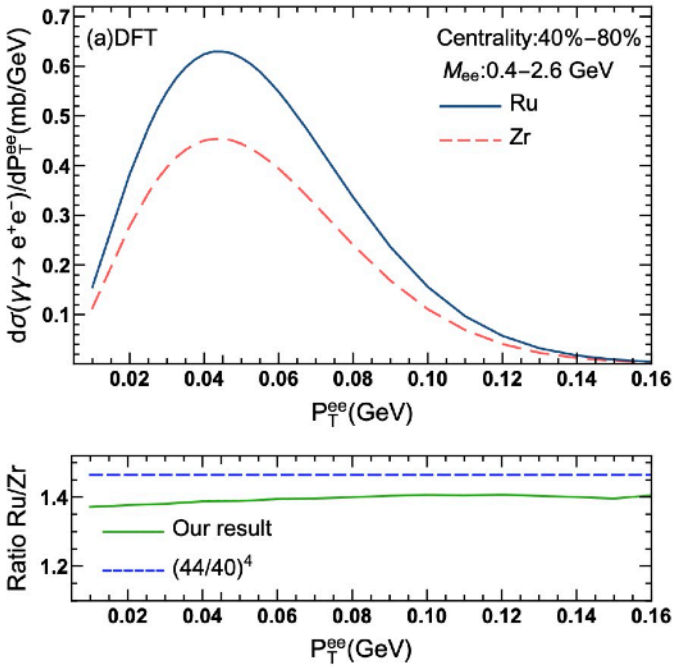

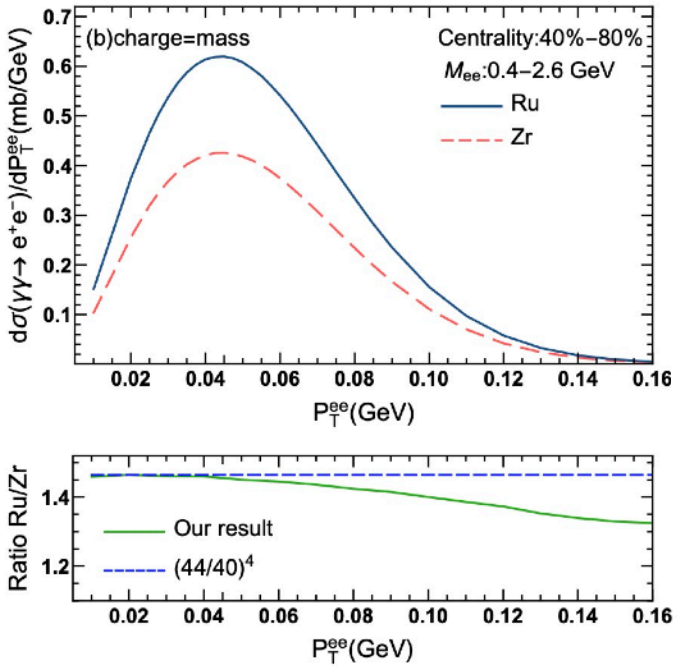

The Born-level total cross section

$$\sigma = \frac{Z^4e^4}{2\gamma^4 v^3}\int d^2\mathbf{b}_T d^2\mathbf{b}_{1T} d^2\mathbf{b}_{2T}\int \frac{d\omega_1 d^2\mathbf{p}_{1T}}{(2\pi)^3}\frac{d\omega_2 d^2\mathbf{p}_{2T}}{(2\pi)^3}$$
$$\times\int \frac{d^2\mathbf{p}'_{1T}}{(2\pi)^2} e^{-i\mathbf{b}_{1T}\cdot(\mathbf{p}'_{1T}-\mathbf{p}_{1T})}\frac{F^*(-\overline{p}'^2_1)}{-\overline{p}'^2_1}\frac{F(-\overline{p}^2_1)}{-\overline{p}^2_1}$$
$$\times\int \frac{d^2\mathbf{p}'_{2T}}{(2\pi)^2} e^{-i\mathbf{b}_{2T}\cdot(\mathbf{p}'_{2T}-\mathbf{p}_{2T})}\frac{F^*(-\overline{p}'^2_2)}{-\overline{p}'^2_2}\frac{F(-\overline{p}^2_2)}{-\overline{p}^2_2}$$
$$\times\int \frac{d^3k_1}{(2\pi)^3 2E_{k1}}\frac{d^3k_2}{(2\pi)^3 2E_{k2}}(2\pi)^4\delta^{(4)}(\overline{p}_1+\overline{p}_2-k_1-k_2)\,\delta^{(2)}(\mathbf{b}_T-\mathbf{b}_{1T}+\mathbf{b}_{2T})$$
$$\times\sum_{\text{spin of }l,\bar{l}}[u_{1\mu}u_{2\nu}L^{\mu\nu}(\overline{p}_1,\overline{p}_2;k_1,k_2)]\,[u_{1\sigma}u_{2\rho}L^{\sigma\rho*}(\overline{p}'_1,\overline{p}'_2;k_1,k_2)]\,,$$

The cross section only sensitive to the charge density, while the centrality definition depends on the mass density.

II. How to probe neutron skin thickness and nuclear symmetry energy using isobar collisions?

Neutron skin: sensitive probe of symmetry energy

$^{96}_{40}\mathrm{Zr} : (N-Z)/A = 0.167$

$^{96}_{44}\mathrm{Ru} : (N-Z)/A = 0.083$

$\Delta r_{\mathrm{np}}^{\mathrm{Zr}} \gg \Delta r_{\mathrm{np}}^{\mathrm{Ru}}$

DFT(eSHF): State-of-the-art DFT calculation using extended Skyrme-Hartree-Fock (eSHF) model.

Z. Zhang, L. Chen, PRC94, 064326(2016)

$$E(\rho,\delta) = E_0(\rho) + E_{\mathrm{sym}}(\rho)\delta^2 + O(\delta^4); \quad \rho = \rho_n + \rho_p; \quad \delta = \frac{\rho_n - \rho_p}{\rho};$$

Slope parameter :

$$L \equiv L(\rho) = 3\rho \left[\frac{dE_{\mathrm{sym}}(\rho)}{d\rho}\right]_{\rho=\rho_0 \text{ saturation density}} \qquad L(\rho_c) = 3\rho_c \left[\frac{dE_{\mathrm{sym}}(\rho)}{d\rho}\right]_{\rho=\rho_c=0.11\rho_0/0.16}$$

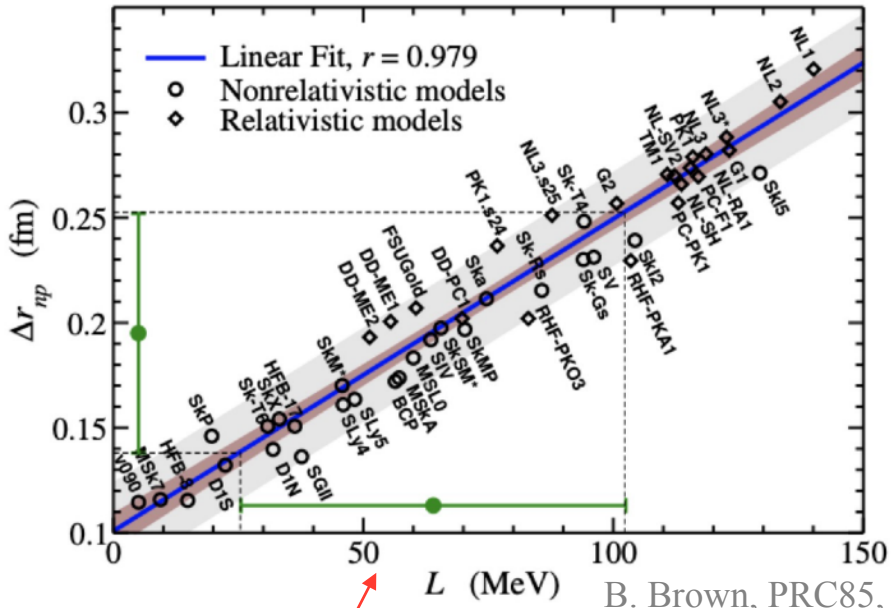

B. Brown, PRC85, 5296 (2000)
R. Furnstahl, NPA, 706, 85 (2002)
X. Roca-Maza, et.al. PRL106, 252501 (2011)

Larger L ⟷ Need small δ to lower E ⟷ Smaller ρ_n, larger Δr

Harder EOS

The symmetry energy is crucial to our understanding of the masses and drip lines of neutron-rich nuclei and the equation of state (EOS) of nuclear and neutron star matter.

Haojie Xu

Current status of neutron skin measurements

PREX-2 Collaboration, PRL126, 172502(2021); B. Reed, et.al., PRL126, 172503(2021)

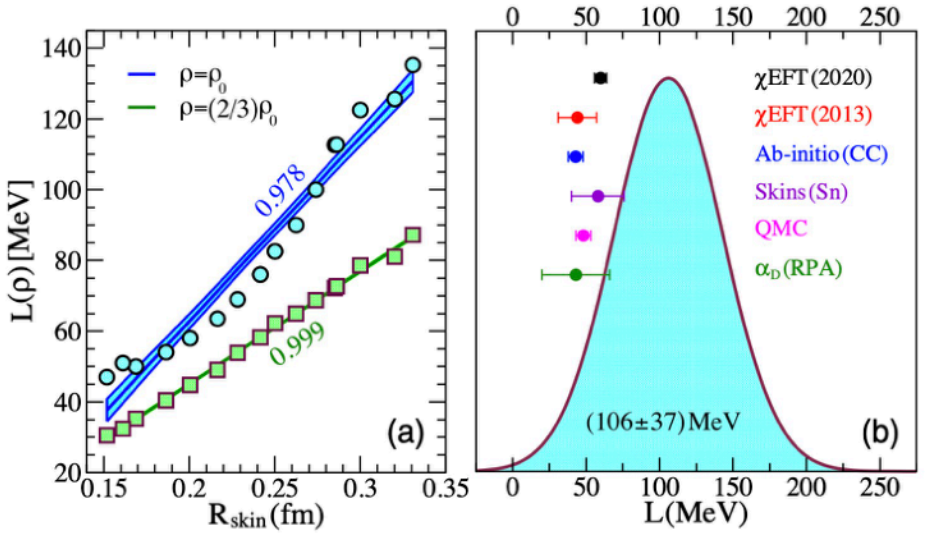

FIG. 1. Left: slope of the symmetry energy at nuclear saturation density ρ_0 (blue upper line) and at $(2/3)\rho_0$ (green lower line) as a function of $R_{\rm skin}^{208}$. The numbers next to the lines denote values for the correlation coefficients. Right: Gaussian probability distribution for the slope of the symmetry energy $L = L(\rho_0)$ inferred by combining the linear correlation in the left figure with the recently reported PREX-2 limit. The six error bars are constraints on L obtained by using different theoretical approaches [14,19–25].

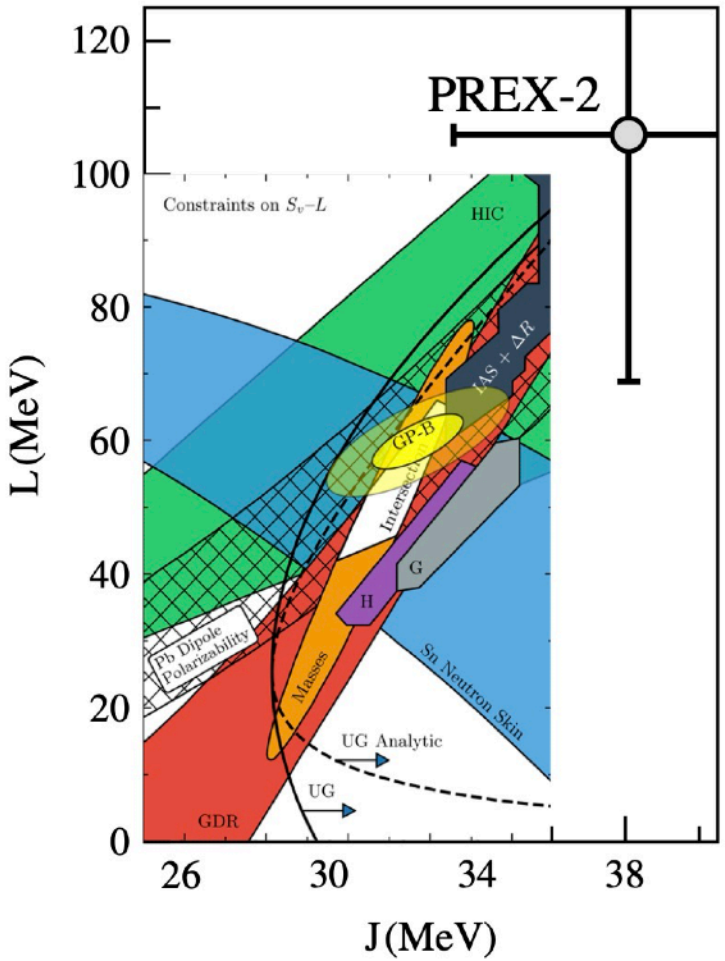

$$\Delta r_{\rm np}^{\rm Pb} = (0.284 \pm 0.071)\ \text{fm}$$

$$L(\rho_0) = (106 \pm 37)\ \text{MeV}$$

$$L(\rho_c) = (71.5 \pm 22.6)\ \text{MeV}$$

This PREX-2 result favors a large neutron skin thickness and symmetry energy slope parameter, at tension with existing experimental data and theoretical analyses.

Haojie Xu

Neutron skin and nuclear symmetry energy

Z. Zhang, PRC94, 064326(2016)
H. Li, HJX, et.al., PRL125, 222301(2020)

SHF: Standard Skyrme-Hartree-Fock (SHF) model
eSHF: Extended SHF model

$$
\begin{aligned}
v_{i,j} &= t_0(1+x_0P_\sigma)\delta(\boldsymbol{r}) + \frac{1}{6}t_3(1+x_3P_\sigma)\rho^\alpha(\boldsymbol{R})\delta(\boldsymbol{r}) \\
&+ \frac{1}{2}t_1(1+x_1P_\sigma)[K'^2\delta(\boldsymbol{r}) + \delta(\boldsymbol{r})K^2] \\
&+ t_2(1+x_2P_\sigma)\boldsymbol{K}'\cdot\delta(\boldsymbol{r})\boldsymbol{K} \\
&+ \frac{1}{2}t_4(1+x_4P_\sigma)[K'^2\delta(\boldsymbol{r})\rho(\boldsymbol{R}) + \rho(\boldsymbol{R})\delta(\boldsymbol{r})K^2] \\
&+ t_5(1+x_5P_\sigma)\boldsymbol{K}'\cdot\rho(\boldsymbol{R})\delta(\boldsymbol{r})\boldsymbol{K} \qquad \text{Extended} \\
&+ iW_0(\boldsymbol{\sigma}_i+\boldsymbol{\sigma}_j)\cdot[\boldsymbol{K}'\times\delta(\boldsymbol{r})\boldsymbol{K}], \qquad (4)
\end{aligned}
$$

$$E(\rho,\delta) = E_0(\rho) + E_{\rm sym}(\rho)\delta^2 + O(\delta^4)$$

$$\rho = \rho_n + \rho_p;\ \ \delta = \frac{\rho_n - \rho_p}{\rho}$$

$$L(\rho_c) = 3\rho_c\left[\frac{dE_{\rm sym}(\rho)}{d\rho}\right]_{\rho=\rho_c};\ \ \rho_c \simeq 0.11\text{fm}^{-3}$$

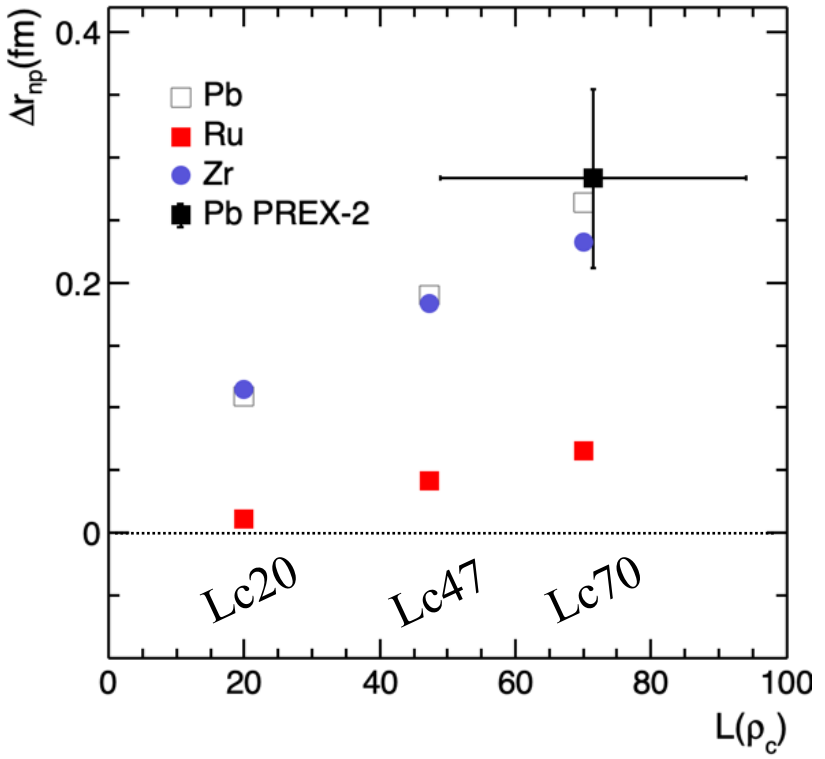

			^{96}Zr			^{96}Ru			^{208}Pb
	$L(\rho_c)$	$L(\rho_0)$	r_n	r_p	$\Delta r_{\rm np}$	r_n	r_p	$\Delta r_{\rm np}$	$\Delta r_{\rm np}$
Lc20	20	13.1	4.386	4.27	0.115	4.327	4.316	0.011	0.109
Lc47	47.3	55.7	4.449	4.267	0.183	4.360	4.319	0.042	0.190
Lc70	70	90.0	4.494	4.262	0.232	4.385	4.32	0.066	0.264
SLy4	42.7	46.0	4.432	4.271	0.161	4.356	4.327	0.030	0.160

Method I: multiplicity distribution ratio

H. Li, HJX, et.al., PRL125, 222301(2020)

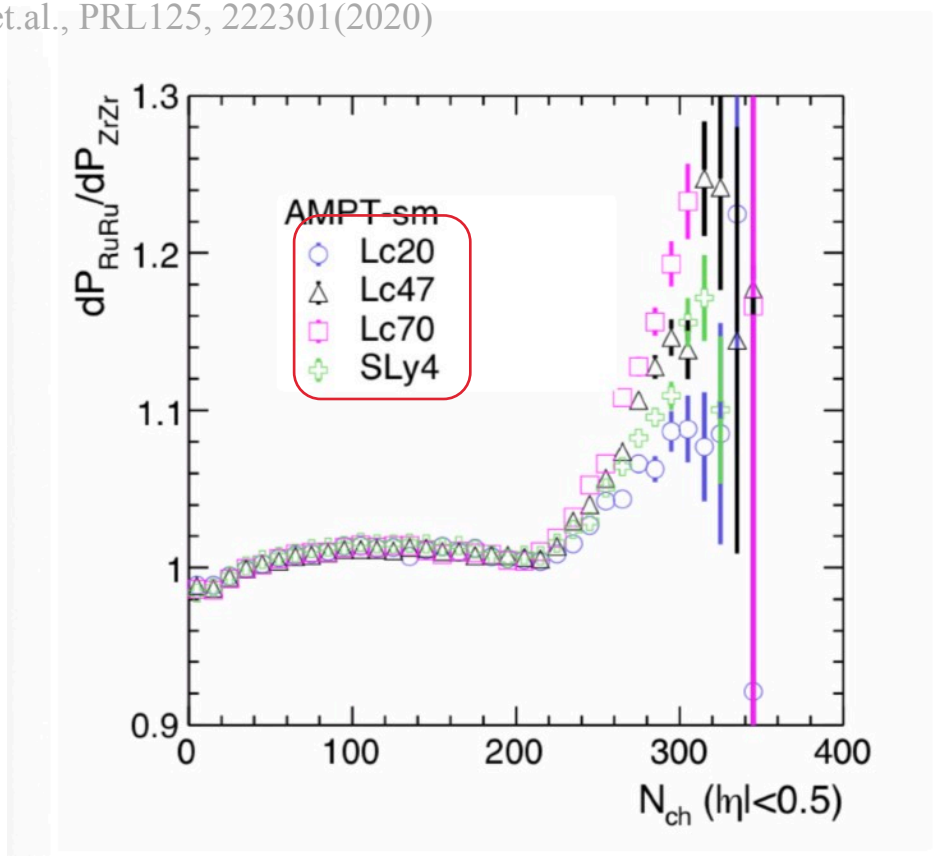

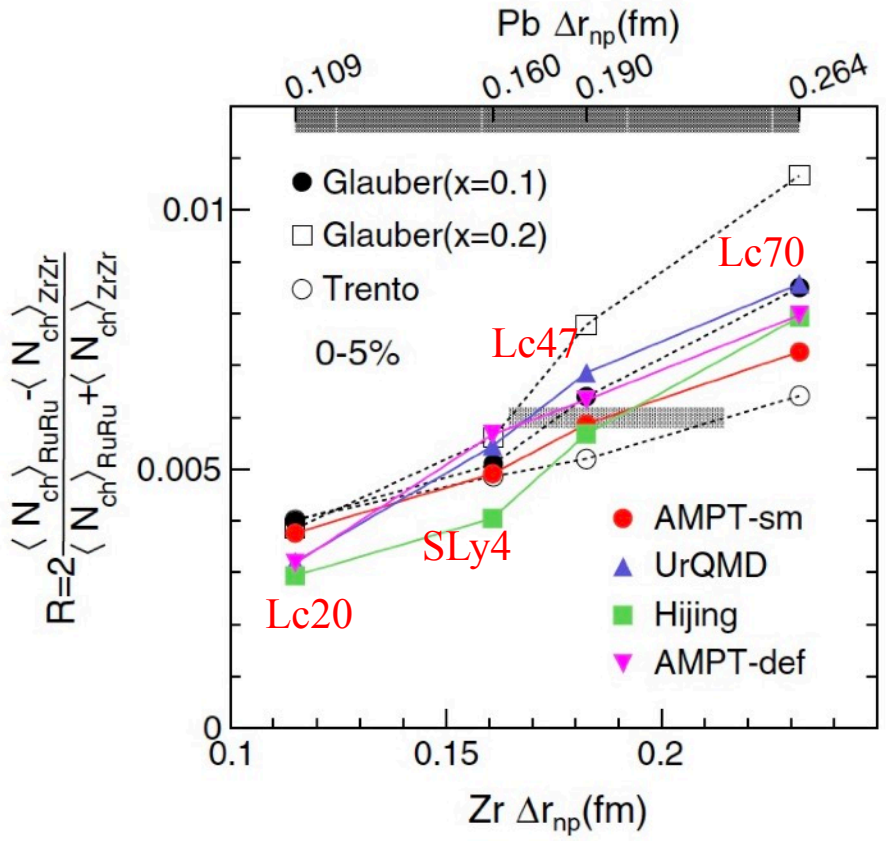

- The ratio of N_{ch} distributions highlight the differences
- To quantify the differences, we use the R observable of N_{ch} at top 5% centrality.
- R is a relative measure, **much of experimental effects cancel**

Method II: mean p_T ratio

HJX, et.al, arXiv:2111.14812

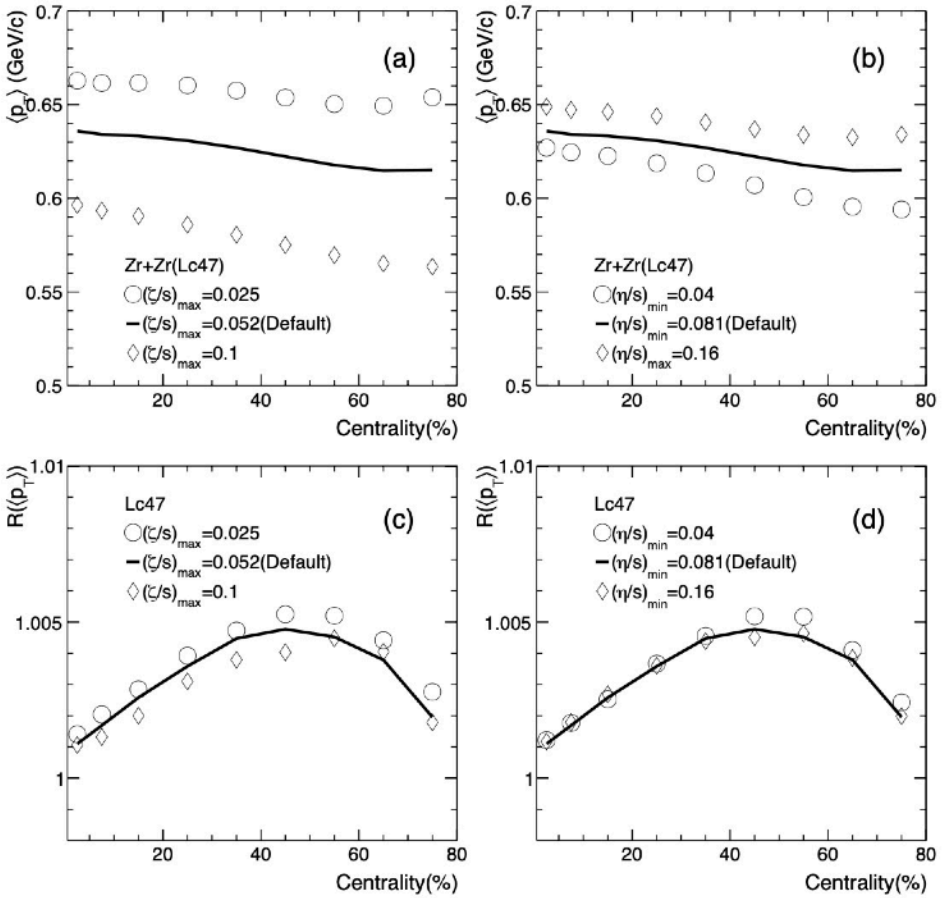

$$R(\langle p_T \rangle) \propto R(d_\perp) \propto 1/R(\langle \sqrt{r^2} \rangle)$$

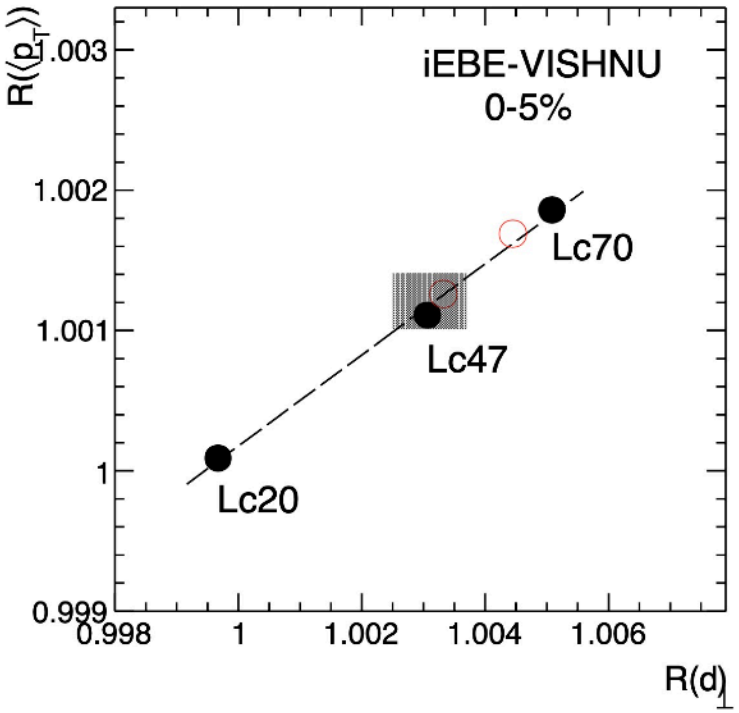

The $R(\langle p_T \rangle)$ is inversely proportional to nuclear size ratio in most central collisions.

Haojie Xu

STAR measurements

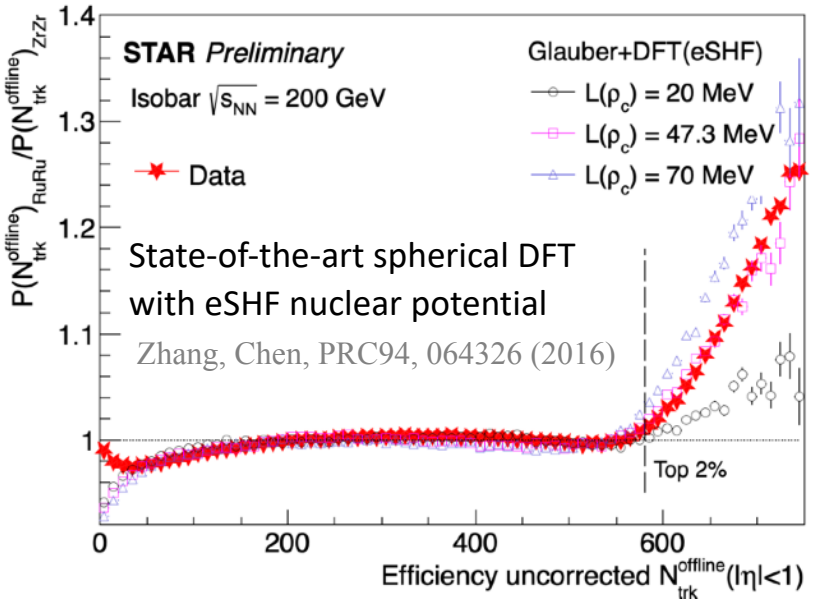

State-of-the-art spherical DFT with eSHF nuclear potential

Zhang, Chen, PRC94, 064326 (2016)

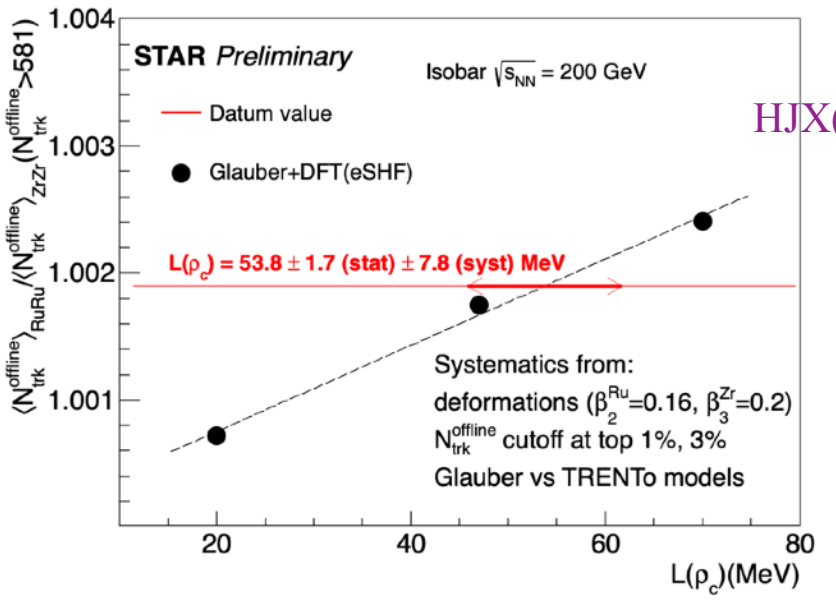

HJX(STAR), QM2022

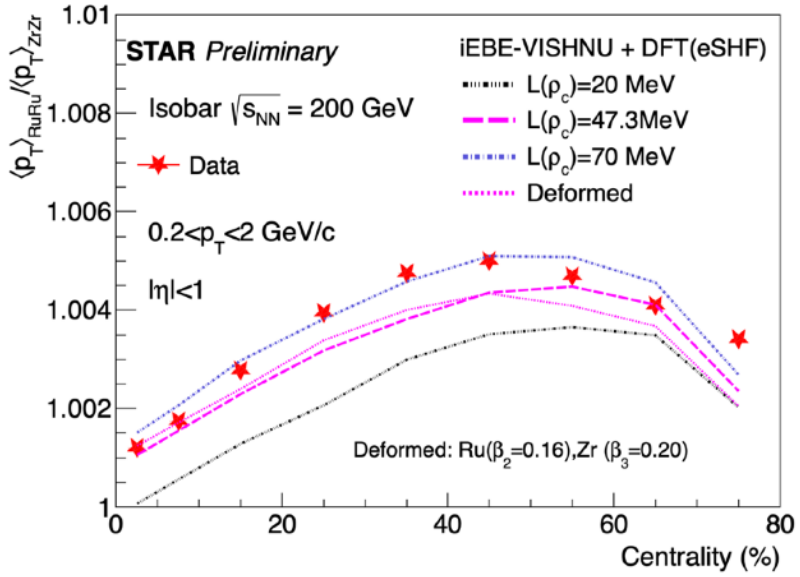

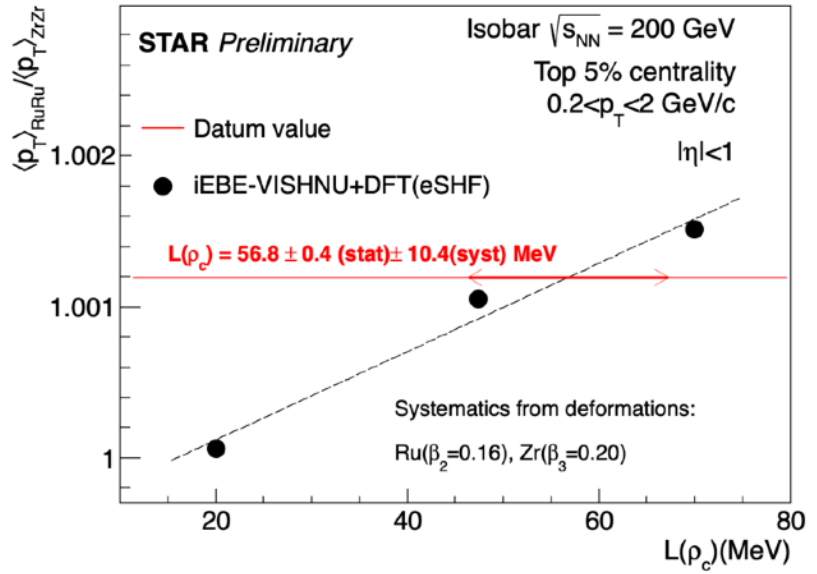

Lc (MeV)	L (MeV)
20	13.1
47.3	55.7
70	90

Haojie Xu

STAR measurements

Compare to world wide data

State-of-the-art **spherical** DFT with eSHF nuclear potential

Zhang, Chen, PRC94, 064326 (2016)

- Multiplicity ratio:

$L(\rho_c) = 53.8 \pm 1.7 \pm 7.8$ MeV

$L(\rho) = 65.4 \pm 2.1 \pm 12.1$ MeV

$\Delta r_{\mathrm{np,Zr}} = 0.195 \pm 0.019$ fm

$\Delta r_{\mathrm{np,Ru}} = 0.051 \pm 0.009$ fm

- $\langle p_T \rangle$ ratio:

$L(\rho_c) = 56.8 \pm 0.4 \pm 10.4$ MeV

$L(\rho) = 69.8 \pm 0.7 \pm 16.0$ MeV

$\Delta r_{\mathrm{np,Zr}} = 0.202 \pm 0.024$ fm

$\Delta r_{\mathrm{np,Ru}} = 0.052 \pm 0.012$ fm

B. Li, et.al Universe 7, 182 (2021)

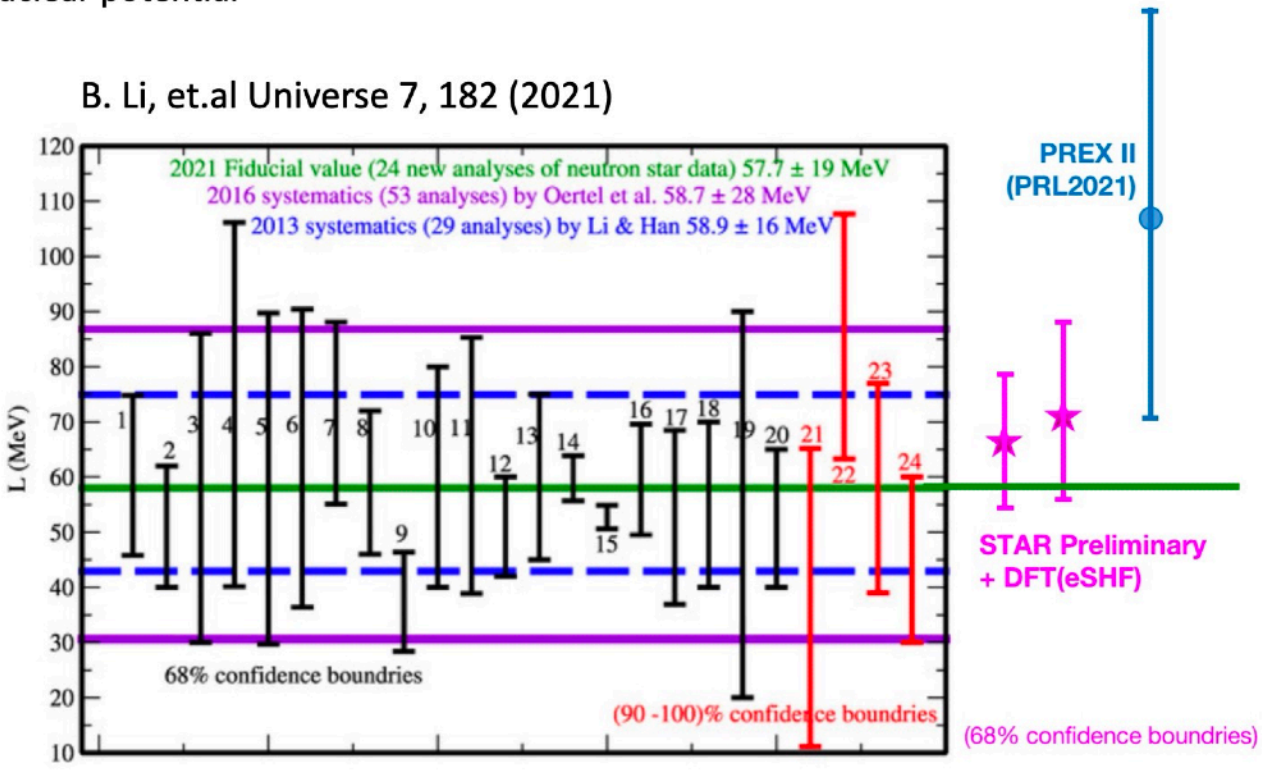

Consistent with world wide data with good precision

Haojie Xu

Method III: net-charge ratio in very peripheral collisions

α is the ΔQ ratio in nn to pp interaction:

Pytha: $\alpha = -0.352$

Hijing: $\alpha = -0.389$

UrQMD: $\alpha = -0.344$

HJX, et.al., PRC105, L011901 (2022)

For the colliding nuclei with large neutron skin thickness

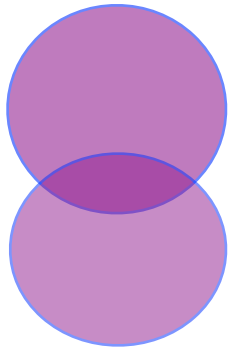

more n+n collisions at most peripheral collisions; Less participant charges, thus less final net-charges

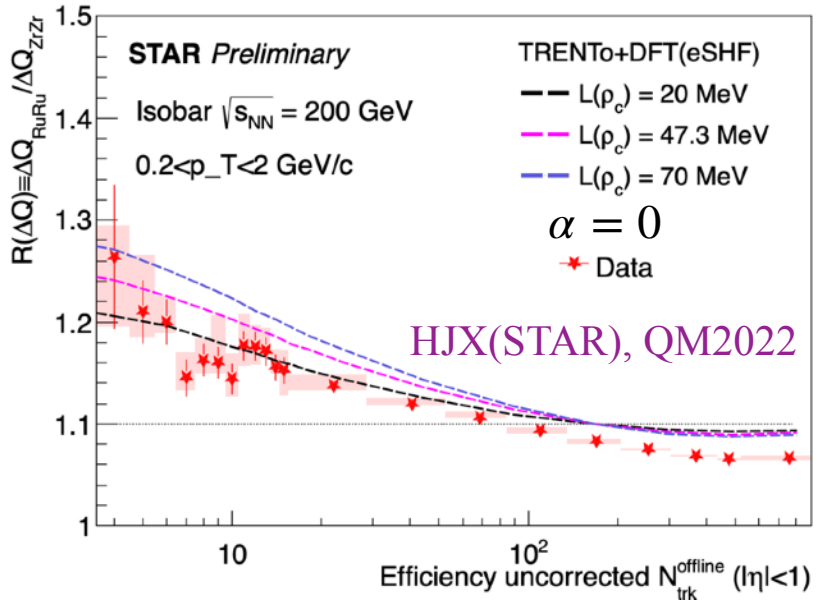

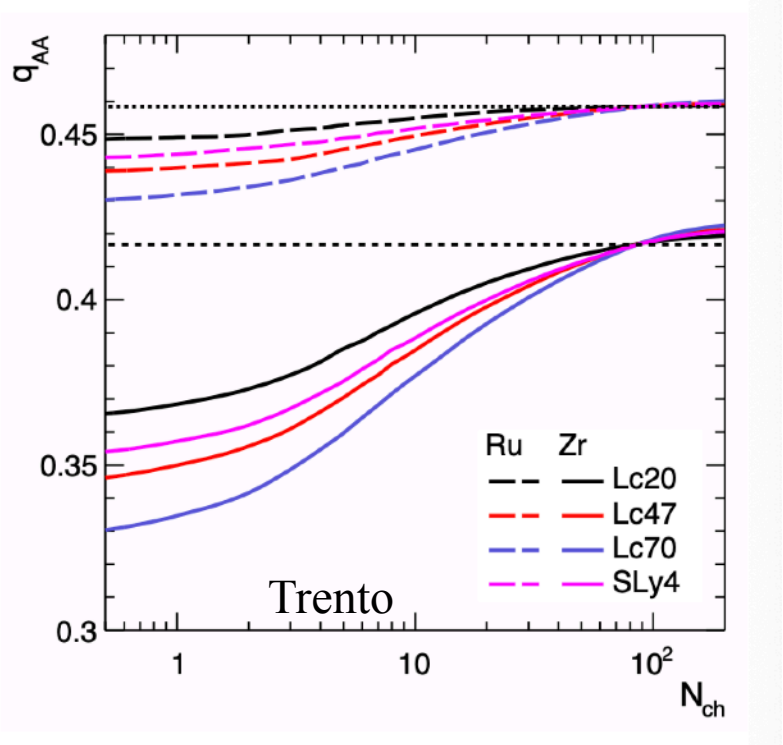

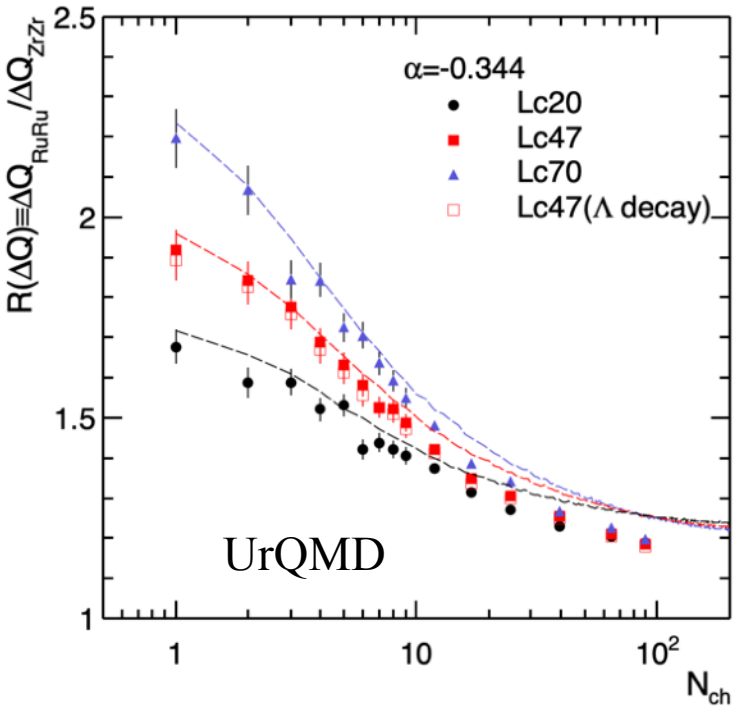

The curves are calculated by superimposition assumption

$$R(\Delta Q) = \frac{q_{RuRu}+\alpha/(1-\alpha)}{q_{ZrZr}+\alpha/(1-\alpha)}$$

where $q_{RuRu/ZrZr}$ are the fraction of protons among the participant nucleons, obtained by the Trento model.

Haojie Xu

Method IV: spectator neutrons in ultracentral collisions

L. Liu, et.al, PLB834, 137441(2022)

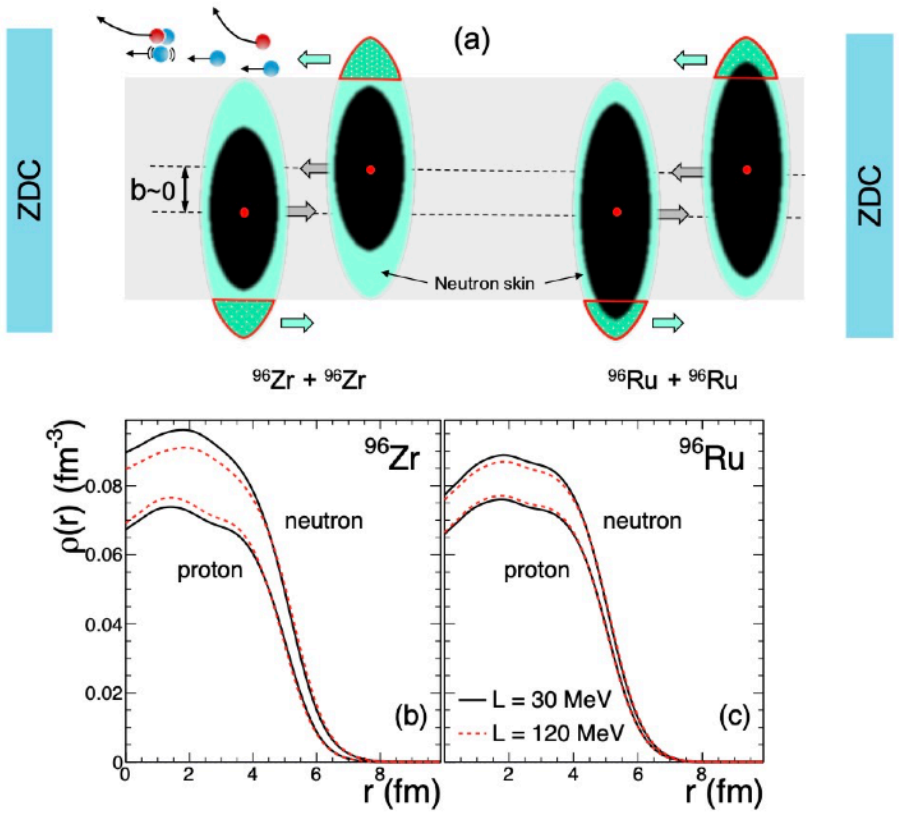

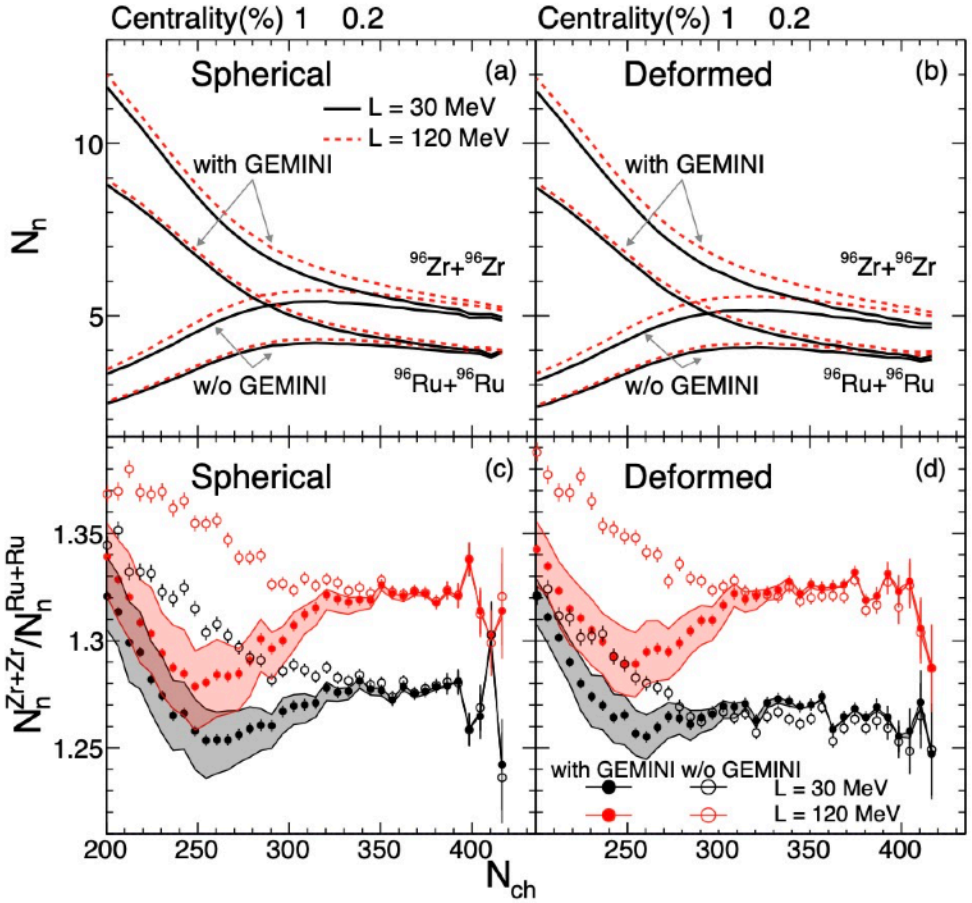

The yield ratio of free spectator neutrons is a clean probe of the neutron-skin thickness

Haojie Xu

Nuclear deformation

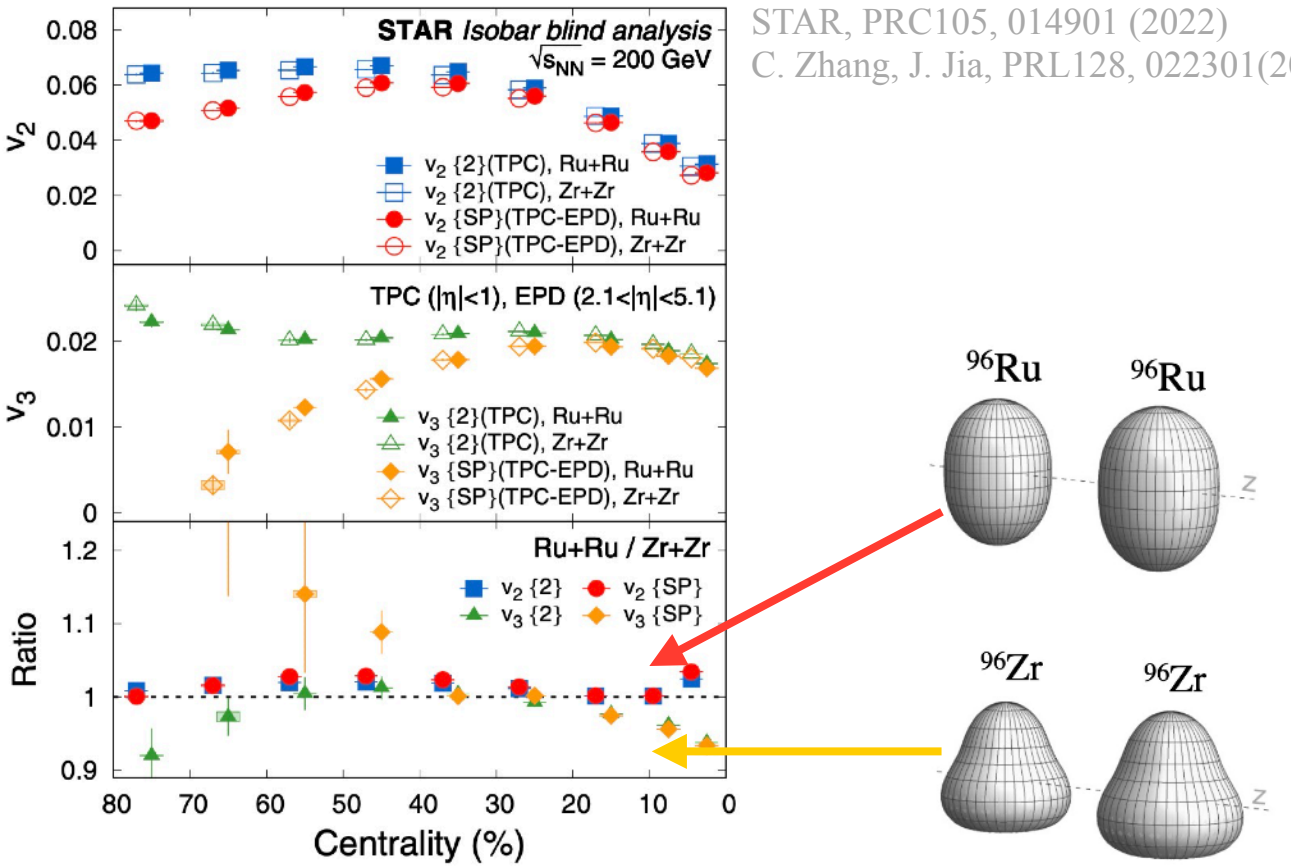

STAR, PRC105, 014901 (2022)
C. Zhang, J. Jia, PRL128, 022301(2022)

Jiangyong Jia's talk

S. Zhao, HJX, et.al, arXiv:2204.02387

$$\mathrm{ac}_2\{3\} \equiv \langle\langle e^{i(2\varphi_1+2\varphi_2-4\varphi_3}\rangle\rangle = \langle v_2^2 v_4 \cos 4(\Psi_2-\Psi_4)\rangle$$

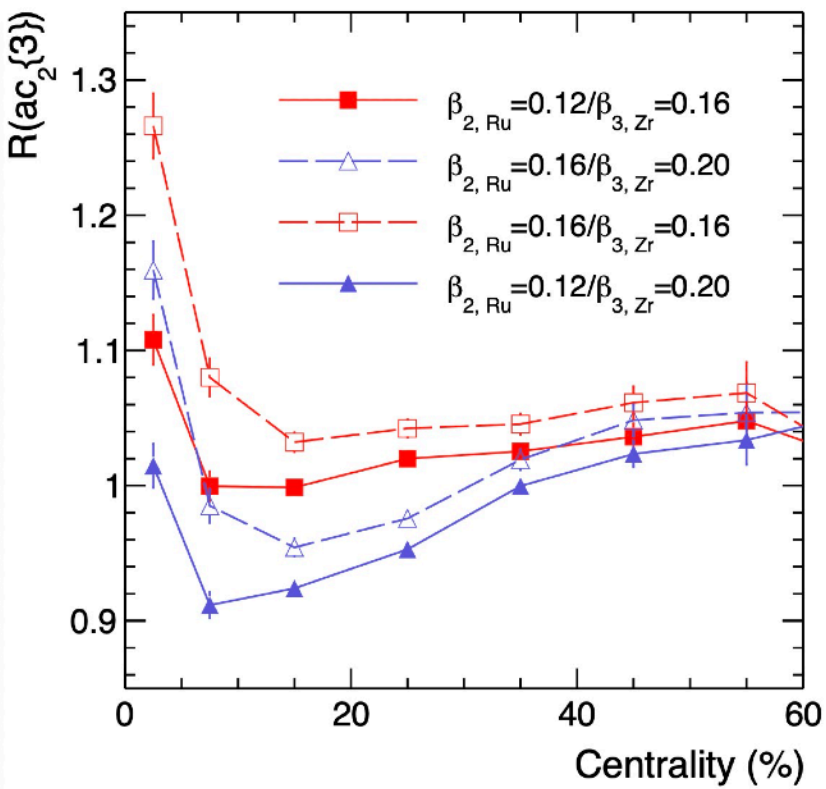

Sizable v_2 and v_3 ratios in central collisions indicate **shape difference between isobars**

SUMMARY

- The STAR isobar data indicate **thick halo-type neutron skin in Zr**, consistent with **DFT** calculations
  - Nuclear structure causes isobar multiplicity and v2 differences, important for the CME search
- Precision isobar data can be used to **probe the neutron skin and symmetry energy**
  - Multiplicity distribution ratio; Mean p_T ratio; Net charge ratio; Spectator proton ratio,…

Thank you for your attention!

Haojie Xu(徐浩洁)

Huzhou University(湖州师范学院)